On string vibrations influenced by a smooth obstacle at one of the endpoints

Ihsan, A.F.; van Horssen, W. T.; Tuwankotta, J.M.

DOI
10.1016/j.jsv.2024.118311

Publication date
2024

Document Version
Final published version

Published in
Journal of Sound and Vibration

Journal of Sound and Vibration 576 (2024) 118311

Contents lists available at ScienceDirect

Journal of Sound and Vibration

journal homepage: www.elsevier.com/locate/jsvi

On string vibrations influenced by a smooth obstacle at one of the endpoints

A.F. Ihsan [a], W.T. van Horssen [b], J.M. Tuwankotta [c,*]

[a] School of Computing, Telkom University, Indonesia
[b] Delft Institute of Applied Mathematics, Delft University of Technology, Netherlands
[c] Faculty of Mathematics and Natural Sciences, Institut Teknologi Bandung, Indonesia

ARTICLE INFO

Keywords:
Moving boundary problem
Characteristic coordinates
Modal interactions
Multiple time-scales perturbation method

ABSTRACT

In this paper, the vibrations of a string are considered. At one end of the string, a smooth obstacle is placed and the other end of the string is attached to a fixed point. The contact between the string and the obstacle varies in time, and leads to a linear, moving boundary value problem for the string vibrations. By applying a boundary fixing transformation, the problem is transformed from a linear problem with a moving boundary, to a nonlinear problem with fixed boundaries. It is assumed that the vibrations around the stationary position of the string are small. Explicit approximations of the solution are obtained by using a multiple time-scales perturbation method. Depending on the parameters in the problem, it turns out that three different cases for the obstacle boundary condition have to be considered, that is, Dirichlet, or Neumann, or Robin type of boundary conditions. To avoid an infinite-dimensional system of ordinary differential equations that occurs in the analysis of the modal interactions of the string vibrations, characteristic coordinates are used together with a multiple time-scales approach to analyze the string dynamics in terms of traveling waves in opposite directions. A comparison between a direct numerical integration of the PDE problem and the results obtained by using the aforementioned perturbation approach shows an excellent agreement in the results.

1. Introduction

Problems for one dimensional string vibrations are classical problems and are studied intensively since the 18th century. In its simplest form, the string is attached to fixed endpoints. However, in some applications for musical instruments, a smooth obstacle may be present at one endpoint of the string, causing the contact of the string to the obstacle to change in time. This leads to a moving boundary problem for the wave equation.

A lot of research in the past has been done to study string vibrations with moving boundaries. One of the initial studies is done by Balazs [1] who considered a wave problem with constantly expanding domain. In the case of musical instruments, where the presence of an obstacle disturbs the vibrations, some studies are using a modal approach [2], general integral transforms [3], and d'Alembert's formula [4] to investigate the problem. These kind of problems have also been studied as phenomena for collisions between a string and an obstacle (see [5,6]). However, these studies considered the obstacle position to be in the middle of the domain. Whereas for the musical instruments, the obstacle is positioned at one of the boundaries. Vyasarayani et al. [7] considered a model for a Sitar instrument. Mandal and Wahi studied this model in terms of its vibration modes [8] and the occurring mode-locking

* Corresponding author.
E-mail address: jmtuwankotta@itb.ac.id (J.M. Tuwankotta).

https://doi.org/10.1016/j.jsv.2024.118311
Received 2 October 2023; Received in revised form 26 January 2024; Accepted 26 January 2024
Available online 27 January 2024

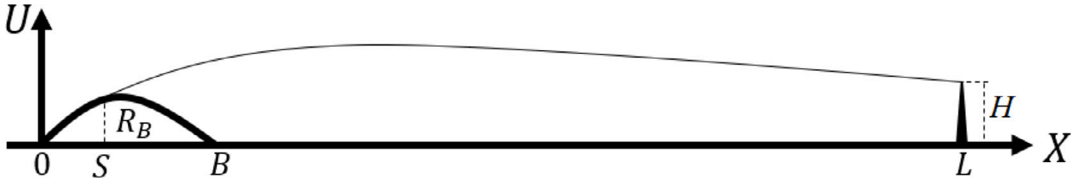

Fig. 1. Illustration of the model.

phenomena [9]. The problem can be extended to consider vibrations in other dimensions as doubly curved obstacles are considered (see [10,11]).

In this study, we consider a generalization of the problem derived by Vyasaravani et al. [7]. While many studies about constrained string vibration consider the obstacle to be parabolic-shaped (see [2,8–12]), we take more general shapes for the obstacle with some additional curvature properties. In case of a parabolic obstacle, our study here is some sort of refinement of the work of Mandal and Wahi [8] with somewhat different approaches. In [8], the solution is assumed to take a specific form without proof. This paper provides a rigorous mathematical derivation of the solution and validates the assumptions made in [8]. Furthermore, we construct a diagram in the parameter space to indicate different types of boundary conditions depending on the parameters. This diagram in the parameter space provides a good insight in the relation between the physical parameters and the type of simplified boundary conditions, which are used as approximations. Lastly, we propose an analysis using characteristic coordinates. Implementation of this approach has the benefit of avoiding truncation problems in the infinite series representations for the solutions, which is notorious in problems described by wave equations.

We organized this paper as follows. In Section 2, some transformations are introduced which are used to reformulate the problem in a nonlinear problem for a fixed domain. In Section 3, the dependence on the moving boundary variable will be removed to obtain a general form for a nonlinear boundary value problem. We also provide a derivation of the problem for some specific examples of obstacle shapes. In the further analysis of the problem, we focus specifically on the problem with a parabolic obstacle.

In Section 4, we apply first a naive perturbation method to obtain an approximate solution, which confirms what has been obtained in [8]. To further refine the approximations on longer time-scales, we also apply a two time-scales perturbation method to the problem. By eliminating so-called secular terms in the higher order problems, we obtain corrections to the solution of the lower order problems, which will be also dependent on the slow-time variable. However, we will arrive at an infinite-dimensional system of modal interactions. This infinite-dimensional system cannot be truncated because all modes are interacting. In that case, characteristic coordinates are used as an alternative (see also for instance [13]). As in [13] it is shown in Appendix A of this paper that this infinite Fourier series approach and the approach with characteristic coordinates are equivalent when one wants to remove secular terms in the approximations. In Section 5, a system of traveling waves obtained by the characteristic coordinate approach will be solved numerically to obtain the complete dynamics of the problem. We also compare these results with the approximations obtained from the naive perturbation expansions. Finally, in Section 6 of this paper, we draw some conclusions.

2. Model formulation for general obstacle problem

Consider a horizontal domain with length L. Let us denote the horizontal axis along this domain as X. At $x = 0$, an obstacle of length B is placed with geometry defined by a continuously differentiable function $R_B(X)$ that satisfies (i) $R_B(0) = R_B(B) = 0$, (ii) $R_B(X) > 0$ at $0 < X < B$, and (iii) $R_B(X)$ has exactly one point at $0 < X < B$ where its first derivative is zero. At $x = L$, the string is attached to a point of height H from the horizontal axis. The value of H is not restricted to have only positive values.

A string with tension T and length-density ρ is then attached to the left-side of the obstacle, and to the tip of the right holder at the other end. The displacement of the string from the horizontal axis will be denoted as U. It is assumed that the string is only attached to the obstacle for $0 \le X < S(\bar{\tau}) < B$, where $S(\bar{\tau})$ is an unknown function, which depends on the vibrations of the string. Here, $\bar{\tau}$ is time. The illustration of this problem is shown in Fig. 1.

The dynamics of the string is governed by the following wave equation:

$$U_{\bar{\tau}\bar{\tau}} - \frac{T}{\rho} U_{XX} = 0, \qquad S(\bar{\tau}) < X < L, \quad \bar{\tau} > 0. \tag{1a}$$

The string satisfies the following boundary conditions:

$$U(S(\bar{\tau}), \bar{\tau}) = R_B(S(\bar{\tau})), \qquad \bar{\tau} > 0, \tag{1b}$$

$$U(L, \bar{\tau}) = H, \qquad \bar{\tau} > 0, \tag{1c}$$

$$U_X(S(\bar{\tau}), \bar{\tau}) = {R_B}'(S(\bar{\tau})), \qquad \bar{\tau} > 0. \tag{1d}$$

where the prime indicates differentiation with respect to its argument. Initially, the displacement and the velocity of the strings are:

$$U(X, 0) = F(X), \qquad R_B(S(0)) < X < L, \tag{1e}$$

$$U_{\bar{\tau}}(X, 0) = G(X), \qquad R_B(S(0)) < X < L. \tag{1f}$$

We introduce first some transformations.

2.1. Dimensionless variables and reduction of parameters

We define a new set of dimensionless variables:

$$\bar{x} = \frac{X}{L}, \quad \bar{u}(\bar{x},\tau) = \frac{U(X,\bar{\tau})}{L}, \quad \tau = \bar{\tau}\sqrt{\frac{T}{\rho L^2}}, \quad s(\tau) = \frac{S(\bar{\tau})}{L},$$
$$r_b(\bar{x}) = \frac{R_B(X)}{L} \quad \bar{f}(\bar{x}) = \frac{F(X)}{L}, \quad \bar{g}(\bar{x}) = \frac{G(X)}{L}\sqrt{\frac{\rho L^2}{T}},$$

and parameters:

$$a = \frac{H}{L}, \qquad b = \frac{B}{L}.$$

Substituting these parameters and dimensionless variables into (1a)–(1f), one obtains:

$$\bar{u}_{\bar{x}\bar{x}}(\bar{x},\tau) = \bar{u}_{\tau\tau}(\bar{x},\tau), \qquad s(\tau) < \bar{x} < 1, \quad \tau > 0, \tag{2a}$$
$$\bar{u}(s(\tau),\tau) = r_b(s(\tau)), \qquad \tau > 0, \tag{2b}$$
$$\bar{u}(1,\tau) = a, \qquad \tau > 0, \tag{2c}$$
$$\bar{u}_{\bar{x}}(s(\bar{\tau}),\bar{\tau}) = r_b'(s(\tau)), \qquad \tau > 0, \tag{2d}$$
$$\bar{u}(\bar{x},0) = \bar{f}(\bar{x}), \qquad s(\tau) \le \bar{x} \le 1, \quad \tau > 0, \tag{2e}$$
$$\bar{u}_\tau(\bar{x},0) = \bar{g}(\bar{x}), \qquad s(\tau) \le \bar{x} \le 1, \quad \tau > 0. \tag{2f}$$

It can be seen now from (2a)–(2f) that the problem only depends on two independent parameters, i.e. a and b. Furthermore, the problem depends on the shape of the obstacle, and on the initial conditions.

2.2. From a time-dependent spatial interval to a fixed interval

The time-dependent spatial domain can be transformed to a fixed spatial domain in x by introducing the following transformations:

$$x = \frac{\bar{x} - s(\tau)}{1 - s(\tau)}, \quad u(x,\tau) = \bar{u}(\bar{x},\tau), \quad f(x) = \bar{f}(\bar{x}), \quad g(x) = \bar{g}(\bar{x}) + \bar{f}_{\bar{x}}(\bar{x})\frac{s'(0)(1-\bar{x})}{1-s(0)}.$$

Substituting this transformation into (2a)–(2f) yields

$$\left[1 - ((x-1)s'(\tau))^2\right] u_{xx} = (1-s(\tau))^2 u_{\tau\tau} + 2(x-1)(1-s(\tau))s'(\tau)u_{x\tau} + (x-1)\left[2(s'(\tau))^2 + (1-s(\tau))s''(\tau)\right] u_x, \tag{3a}$$

for $0 < x < 1, \tau > 0$, subject to the boundary conditions

$$u(0,\tau) = r_b(s(\tau)), \qquad \tau > 0, \tag{3b}$$
$$u(1,\tau) = a, \qquad \tau > 0, \tag{3c}$$
$$u_x(0,\tau) = (1-s(\tau))r_b'(s(\tau)), \qquad \tau > 0, \tag{3d}$$

and subject to the initial conditions

$$u(x,0) = f(x), \qquad 0 < x < 1, \tag{3e}$$
$$u_\tau(x,0) = g(x), \qquad 0 < x < 1. \tag{3f}$$

3. Removal of the time dependent attachment–detachment point $s(\tau)$ from the problem

To obtain a simpler problem, we will remove $s(\tau)$ explicitly from the problem (3a)–(3f). First we differentiate (3b) with respect to τ to obtain $u_\tau(0,\tau) = r_b'(s(\tau))s'(\tau)$. From this expression and (3d), we can remove $r_b'(s(\tau))$, yielding

$$\frac{u_\tau(0,\tau)}{u_x(0,\tau)} = \frac{1}{1-s(\tau)}s'(\tau)$$

Integrating this expression with respect to τ from $\tau = 0$ to $\tau = \tau$ yields:

$$s(\tau) = 1 - KE(\tau), \tag{4}$$

where

$$W(\tau) = \frac{u_\tau(0,\tau)}{u_x(0,\tau)}, \qquad E(\tau) = \exp\left(-\int_0^\tau W(\theta)d\theta\right),$$

and $K = 1 - s(0)$. To obtain the boundary condition without $s(\tau)$, we substitute (4) into one of the BCs (3b) or (3d). For instance, we take (3b) and we have

$$u(0,\tau) = r_b(1 - KE(\tau)). \tag{5}$$

Now, to obtain a partial differential equation (PDE) without $s(\tau)$, we substitute again the explicit form for $s(\tau)$ given by (4) into (3a) and obtain

$$u_{xx} = (KE(\tau))^2 \left[(x-1)^2 W(\tau)^2 u_{xx} + u_{\tau\tau} + 2W(\tau)(x-1)u_{x\tau} + (x-1)(W(\tau)^2 + W'(\tau))u_x\right]. \tag{6}$$

The PDE (6) with boundary conditions (5) and (3c) forms the problem formulation for the general obstacle problem. In the next subsection, we show how we can derive the explicit problems for some specific choices for $r_b(x)$.

3.1. Some obstacle functions $r_b(x)$ and the corresponding nonlinear BC at $x = 0$

1. A parabolic obstacle: $r_b(x) = x(b - x)$.
   In this case, by using (4) the boundary condition (3b) becomes:
   $$u(0,\tau) = (b-1) + (2-b)KE(\tau) - K^2 E(\tau)^2.$$
   If we solve this for $E(\tau)$, we obtain
   $$E(\tau) = \frac{1}{K}\left(1 - \frac{b}{2} + \sqrt{\frac{b^2}{4} - u(0,\tau)}\right).$$
   From the definition of $E(\tau)$, we have that
   $$\exp\left(-\int_c^\tau \frac{u_\theta(0,\theta)}{u_x(0,\theta)}d\theta\right) = \frac{1}{K}\left(1 - \frac{b}{2} + \sqrt{\frac{b^2}{4} - u(0,\tau)}\right),$$
   and by differentiation with respect to τ one obtains:
   $$-\frac{u_\tau(0,\tau)}{u_x(0,\tau)} = u_\tau(0,\tau)\left(\frac{1}{1 - \frac{b}{2} + \sqrt{\frac{b^2}{4} - u(0,\tau)}}\right)\left(\frac{-1}{2\sqrt{\frac{b^2}{4} - u(0,\tau)}}\right).$$
   After some algebraic manipulations, we obtain the following condition:
   $$\left(2u(0,\tau) + u_x(0,\tau) - \frac{b^2}{2}\right)^2 = 4\left(1 - \frac{b}{2}\right)^2\left(\frac{b^2}{4} - u(0,\tau)\right). \tag{7}$$
   Observe also that by the definition of $E(\tau)$, we have that $W(\tau) = -\frac{\dot{E}(\tau)}{E(\tau)}$. Substituting both $E(\tau)$ and $W(\tau)$ into (6) gives us the following PDE:
   $$\begin{aligned} u_{xx} = {} & \left(\lambda(x-1)\left(2u_\tau(0,\tau) + u_{x\tau}(0,\tau)\right)\right)^2 u_{xx} + (1 - \lambda(b - 2u(0,\tau) - u_x(0,\tau)))^2 u_{\tau\tau} \\ & - 2(x-1)(1 - \lambda(b - 2u(0,\tau) - u_x(0,\tau)))\lambda(2u_\tau(0,\tau) + u_{\tau\tau}(0,\tau))u_{x\tau} + (x-1)\left[2\lambda^2(2u_\tau(0,\tau) + u_{x\tau}(0,\tau))^2\right. \\ & \left. - \lambda(1 - \lambda(b - 2u(0,\tau) - u_x(0,\tau)))(2u_{\tau\tau}(0,\tau) + u_{x\tau\tau}(0,\tau))\right] u_x, \end{aligned} \tag{8}$$
   where $\lambda = \frac{1}{2-b}$.
2. A sinusoidal obstacle: $r_b(x) = A\sin\left(\frac{\pi x}{b}\right)$ for some positive constant A.
   In this case, the boundary condition (3b) and (3d) become
   $$u(0,\tau) = A\sin\left(\frac{\pi(1 - KE(\tau))}{b}\right),$$
   and
   $$u_x(0,\tau) = \frac{A\pi}{b}KE(\tau)\cos\left(\frac{\pi(1 - KE(\tau))}{b}\right).$$
   By using the fact that $\sin^2(\alpha) + \cos^2(\alpha) = 1$, it follows from these BCs that
   $$E(\tau) = \frac{bu_x(0,\tau)}{K\pi\sqrt{A^2 - u^2(0,\tau)}}.$$
   From the definition of $E(\tau)$, we can derive the boundary condition at $x = 0$:
   $$\frac{u_{x\tau}(0,\tau)}{u_\tau(0,\tau)} + \frac{u(0,\tau)u_x(0,\tau)}{A^2 - u^2(0,\tau)} = -1.$$
   Since E and W are now known explicitly, we then also can determine the PDE from (4)–(6) which $u(x,\tau)$ has to satisfy.

3. A half-circular obstacle: $r_b(x) = (x(b-x))^{\frac{1}{2}}$.
   In this case, the boundary condition (3d) becomes
   $$u_x(0,\tau) = \frac{1}{2}\frac{b-2s(\tau)}{u(0,\tau)}.$$
   By using (4), $E(\tau)$ then can be explicitly obtained as
   $$E(\tau) = \frac{1}{K}\left(1 - \frac{1}{4}\left[b + 2 + \sqrt{16u(0,\tau)u_x(0,\tau) + (b-2)^2}\right]\right).$$
   After applying some algebraic manipulations, we obtain the following nonlinear BC:
   $$0 = 4[u(0,\tau)]^4 + 8[u(0,\tau)]^3 u_x(0,\tau) + [u(0,\tau)]^2(4[u_x(0,\tau)]^2 - b^2 - 4b + 4) - 2b^2 u(0,\tau)u_x(0,\tau) + b^2(b-1).$$

In all of the above computations, any choice for positive or negative signs is made based on the values of the parameters.

3.2. The stationary solution

Let $u(x,\tau) = y(x) + \varepsilon v(x,\tau)$, where $y(x)$ is the stationary solution of the problem, $v(x,\tau)$ is the oscillating part, and ε is a small positive parameter representing a measure of the small amplitude oscillations around the equilibrium. We can compute $y(x)$ by the geometry of the problem. The stationary string solution, or equivalently the time τ independent solution of (6), should be a linear function in x. The stationary solution $y(x)$ is then obtained from (3b)–(3d) yielding

$$y(x) = a + (1 - s_y)(x-1){r_b}'(s_y), \tag{9}$$

where s_y follows from

$$r_b(s_y) + (1 - s_y){r_b}'(s_y) - a = 0. \tag{10}$$

This shows how the stationary solution for an arbitrarily shaped obstacle can be obtained. However, Eq. (9) is not the true stationary solution in the sense of the original problem, because the spatial variable x in this case is the transformed variable that depends on $s(\tau)$. We can obtain the true time-independent solution by transforming it back to the original variable by using the stationary attachment point s_y, i.e.

$$\bar{y}(\bar{x}) = a + (\bar{x} - 1){r_b}'(s_y).$$

In the further analysis, we will focus on the case of a parabolic obstacle.

3.3. Approximations of the boundary condition at $x = 0$

For a parabolic shaped obstacle, we consider the PDE (8) subject to the boundary condition (7) at $x = 0$, and the boundary condition (3c) at $x = 1$. From Section 3.2 it follows that the stationary solution in this case is:

$$y(x) = a + (1 - s_y)(b - 2s_y)(x-1).$$

where s_y follows from (10) and is given by:

$$s_y = 1 - \sqrt{1 + a - b}.$$

In this case, we can also derive an additional condition $b(b-1) < a < b$ because $0 < s_y < b$. The boundary value problem for the time-dependent part $v(x,\tau)$ is given by:

$$[1 - ((x-1)\lambda\varepsilon\mathfrak{v}')^2]v_{xx} = (1 - s_y + \lambda\varepsilon\mathfrak{v})^2 v_{\tau\tau} - 2(x-1)(1 - s_y + \lambda\varepsilon\mathfrak{v})\lambda\varepsilon\mathfrak{v}' v_{x\tau}$$
$$+ (x-1)[2\varepsilon(\lambda\mathfrak{v}')^2 - (1 - s_y + \lambda\varepsilon\mathfrak{v})\lambda\mathfrak{v}''] \times ((1 - s_y)(b - 2s_y) + \varepsilon v_x), \tag{11a}$$
$$(2 + b - 4s_y)v(0,\tau) = (2s_y - b)v_x(0,\tau) - \varepsilon\mathfrak{v}^2, \tag{11b}$$
$$v(1,\tau) = 0, \tag{11c}$$

where $\lambda = (2-b)^{-1}$ and $\mathfrak{v}(\tau) = 2v(0,\tau) + v_x(0,\tau)$

If we look at BC (11b), we derive three types of approximate boundary conditions depending on the parameter values of b and a.

1. If the height of the right boundary is equal to the top of the bridge (obstacle), i.e.
   $$a = \frac{b^2}{4} + \mathcal{O}(\varepsilon) \quad \text{or} \quad s_y = \frac{b}{2} + \mathcal{O}(\varepsilon),$$
   then condition (11b) becomes a Dirichlet-type of boundary condition, i.e., $v(0,\tau) = \mathcal{O}(\varepsilon)$.

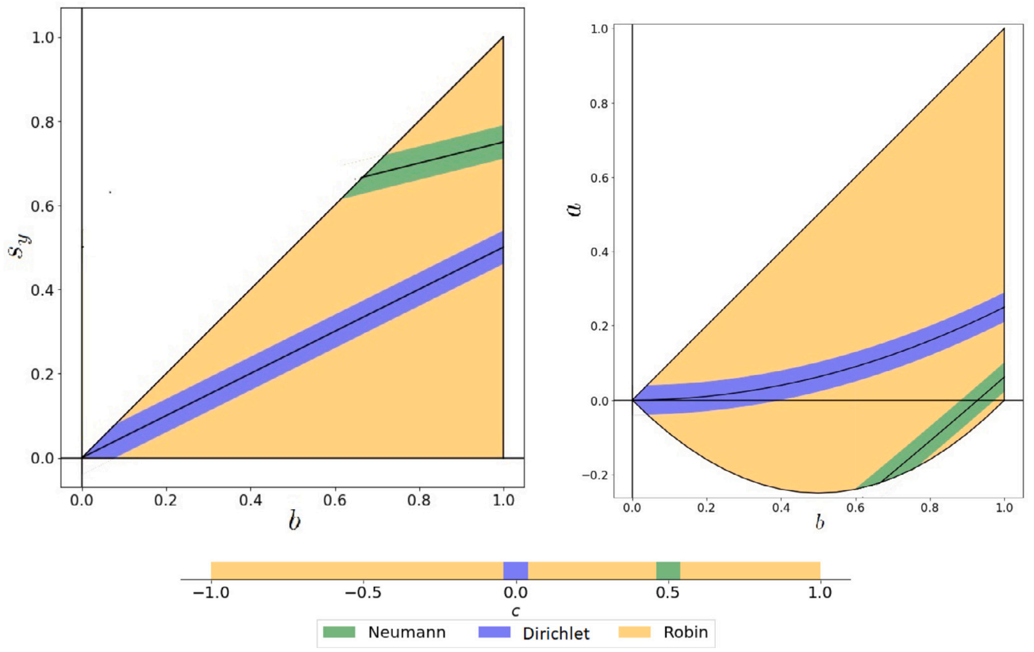

Fig. 2. The separation of regions in the parameter space based on the type of boundary conditions at $x = 0$. The first (upper-left) and second image (upper-right) represent the separation in the (b, s_y) and (b, a) parameter space, respectively. The third image represents separation only in terms of the single parameter c.

2. If

$$a = \frac{b^2}{16} + \frac{3}{4}b - \frac{3}{4} + \mathcal{O}(\varepsilon), \quad \text{or equivalently,} \quad s_y = \frac{b+2}{4} + \mathcal{O}(\varepsilon),$$

then condition (11b) becomes a Neumann-type, i.e., $v_x(0,\tau) = \mathcal{O}(\varepsilon)$. Because $a < \frac{b^2}{4}$, this case implies that the height of the right boundary is lower than the top of the bridge-obstacle. Observe also that in this case $\frac{1}{2} < s_y < b$, so that this condition will be satisfied if $1 > b > \frac{2}{3}$.

3. Otherwise, by default the BC is a Robin-type of boundary condition, i.e.,

$$v_x(0,\tau) = \frac{2 + b - 4s_y}{2s_y - b} v(0,\tau) + \mathcal{O}(\varepsilon).$$

We visualize these separate cases in the parameter space as shown in Fig. 2. These separate cases for the types of boundary condition can be simplified in terms of the new parameter

$$c = \frac{b - 2s_y}{b - 2}. \tag{12}$$

Using this single parameter, the boundary condition becomes $cv_x(0,\tau) = (1-2c)v(0,\tau)$, which is of Dirichlet-type if $c = 0$, of Neumann-type if $c = \frac{1}{2}$, and of Robin-type otherwise.

4. Approximating the solution by means of perturbation method

In this section, we will use perturbation methods to construct approximations of the solutions $v(x,\tau)$ of the initial–boundary value problem (11a)–(11c). We start in Section 4.1 with a naive or straightforward perturbation expansion. Such expansions lead to secular terms in the approximations. For that reason, we will introduce in Section 4.2 a two time-scales perturbation approach. Solving the problem in "Fourier series form" will lead to a system of infinitely many coupled ordinary differential equations. This system cannot be truncated. For that reason, we will introduce in Section 4.3 characteristic coordinates. With this approach the problem can be reduced to a simplified problem, which can (relatively easy) be integrated numerically in Section 5.

4.1. Approximating the solutions by means of perturbation methods

We define the perturbation expansion for v as follows:

$$v(x,\tau) = v^{[0]}(x,\tau) + \varepsilon v^{[1]}(x,\tau) + \mathcal{O}(\varepsilon^2),$$

and $\mathfrak{v}(\tau) = \mathfrak{v}^{[0]}(\tau) + \varepsilon \mathfrak{v}^{[1]}(\tau) + \mathcal{O}(\varepsilon^2)$. We introduce also a time rescaling for simplification: $t = \tau(1 - s_y)$. Substituting these expansions into (11a)–(11c) and collecting the $\mathcal{O}(1)$ terms, we obtain:

$$v^{[0]}_{xx} - v^{[0]}_{tt} = (x-1)\frac{2s_y - b}{2-b}\mathfrak{v}^{[0]}_{tt}, \tag{13a}$$

$$(2 + b - 4s_y)v^{[0]}(0,t) = (2s_y - b)v^{[0]}_x(0,t), \tag{13b}$$

$$v^{[0]}(1,t) = 0. \tag{13c}$$

Problem (13a)–(13c) can be solved directly by using the method of separation of variables. The solution can be written as follows:

$$v(x,t) = \sum_{n=1}^{\infty}\left[C_{1n}\sin\left(\frac{n\pi\tau}{1-s_y}\right) + C_{2n}\cos\left(\frac{n\pi\tau}{1-s_y}\right)\right]\left[\sin(n\pi x) + K_n(x)\right] + \mathcal{O}(\varepsilon), \tag{14}$$

where

$$K_n(x) = \begin{cases} 0, & \text{Dirichlet case;} \\ n\pi(1-x), & \text{Neumann case; and} \\ n\pi\frac{b-2s_y}{2(1-s_y)}(1-x), & \text{Robin case,} \end{cases}$$

and where the constants C_{1n} and C_{2n} are determined by the initial conditions. By using (4) and the approximation for $u(x,\tau)$, we can also obtain the time-dependent part of the moving boundary variable $s(\tau)$, which we will denote as $s_v(\tau)$, where $s(\tau) = s_y + \varepsilon s_v(\tau)$, and

$$s_v(t) = \frac{\pi}{(2-b)(c-1)}\sum_{n=1}^{\infty} n\varphi_n(t) + \mathcal{O}(\varepsilon). \tag{15}$$

Both (14) and (15) derived here lead to the same $\mathcal{O}(1)$-results as obtained in [8]. The difference here is that our solution approach still has higher order terms in ε due to our naive perturbation expansions.

To simplify the problem further, we introduce the transformation (for $i = 0$ and 1):

$$v^{[i]}(x,t) = \tilde{v}^{[i]}(x,t) + \begin{cases} 0, & c = 0, \\ \frac{c(1-x)}{1-c}\left(\tilde{v}^{[i]}_x(0,t) - i\frac{(v^{[0]}(0,t))^2}{(2-b)c^3}\right), & c \neq 0, \end{cases} \tag{16}$$

where c is defined by (12). With this transformation (16), we obtain a problem with homogeneous boundary conditions of Dirichlet-type:

$$\mathcal{O}(1): \quad \tilde{v}^{[0]}_{tt} - \tilde{v}^{[0]}_{xx} = 0, \tag{17a}$$

$$\tilde{v}^{[0]}(0,t) = \tilde{v}^{[0]}(1,t) = 0, \tag{17b}$$

$$\mathcal{O}(\varepsilon): \quad \tilde{v}^{[1]}_{tt} - \tilde{v}^{[1]}_{xx} = \tilde{p}(x,t), \tag{17c}$$

$$\tilde{v}^{[1]}(0,t) = \tilde{v}^{[1]}(1,t) = 0, \ldots, \tag{17d}$$

where

$$\tilde{p}(x,t) = \frac{1}{(1-c)^2(2-b)^2}\left[2\tilde{v}^{[0]}_x(0,t)\tilde{v}^{[0]}_{tt} - (x-1)\left[2\tilde{v}^{[0]}_{xt}(0,t)\tilde{v}^{[0]}_{xt} + \tilde{v}^{[0]}_{xtt}(0,t)\tilde{v}^{[0]}_x\right]\right]$$

for given parameters $c \in (-1,1)$ and $b \in (0,1)$. For simplicity we introduce the parameter λ defined by:

$$\lambda = \frac{1}{(1-c)^2(2-b)^2}.$$

Since the straightforward perturbation expansions lead to unbounded (or secular) terms in $\tilde{v}^{[1]}$, we now introduce the two time-scales perturbation method.

4.2. The two time-scales perturbation expansions

We introduce two time variables $t_0 = t$ and $t_1 = \varepsilon t$, and $\tilde{v} = \tilde{v}(x,t_0,t_1)$ can be expanded in $\tilde{v}^{[0]}(x,t_0,t_1) + \varepsilon\tilde{v}^{[1]}(x,t_0,t_1) + \mathcal{O}(\varepsilon^2)$. The problem then becomes

$$\mathcal{O}(1): \quad \tilde{v}^{[0]}_{t_0t_0} - \tilde{v}^{[0]}_{xx} = 0,$$

$$\tilde{v}^{[0]}(0,t_0,t_1) = \tilde{v}^{[0]}(1,t_0,t_1) = 0,$$

$$\mathcal{O}(\varepsilon): \quad \tilde{v}^{[1]}_{t_0t_0} - \tilde{v}^{[1]}_{xx} = \tilde{p}(x,t_0,t_1),$$

$$\tilde{v}^{[1]}(0,t_0,t_1) = \tilde{v}^{[1]}(1,t_0,t_1) = 0,$$

where $\bar{p}(x,t_0,t_1) = 2\tilde{v}^{[0]}_{t_0t_1} + \tilde{p}(x,t_0,t_1)$. By using the method of separation of variables, we can solve the $\mathcal{O}(1)$ problem and the solution is given by:

$$\tilde{v}^{[0]}(x,t_0,t_1) = \sum_{n=1}^{\infty} \sin(n\pi x)\phi_n^{[0]}(t_0,t_1), \tag{18}$$

where $\phi_n^{[0]}(t_0,t_1) = A_n(t_1)\sin(n\pi t_0) + B_n(t_1)\cos(n\pi t_0)$. The still arbitrary functions $A_n(t_1)$ and $B_n(t_1)$ can be used to eliminate secular terms in the equation of the $\mathcal{O}(\varepsilon)$-problem. Using the method of separation of variables, we write the solution of the $\mathcal{O}(\varepsilon)$ problem as

$$\tilde{v}^{[1]}(x,t_0,t_1) = \sum_{n=1}^{\infty} \sin(n\pi x)\phi_n^{[1]}(t_0,t_1).$$

Substituting this series into the $\mathcal{O}(\varepsilon)$-problem gives us

$$\frac{\partial^2}{\partial t_0^2}\phi_k^{[1]}(t_0,t_1) + (k\pi)^2\phi_k^{[1]}(t_0,t_1) = -2\hat{p}_k(t_0,t_1),$$

where

$$\hat{p}_k(t_0,t_1) = \frac{\partial^2\phi_k^{[0]}}{\partial t_0\partial t_1} + \lambda\sum_{n=1}^{\infty} n\pi\left[\left(\frac{1}{2}\frac{\partial\phi_n^{[0]}}{\partial t_0}\frac{\partial\phi_k^{[0]}}{\partial t_0} - \pi^2\left(k^2+\frac{n^2}{4}\right)\phi_n^{[0]}\phi_k^{[0]}\right) - \sum_{m\neq k}^{\infty}\frac{km}{(m^2-k^2)}\left(2\frac{\partial\phi_n^{[0]}}{\partial t_0}\frac{\partial\phi_m^{[0]}}{\partial t_0} - n^2\pi^2\phi_n^{[0]}\phi_m^{[0]}\right)\right].$$

For now, we are not interested to find the complete solution $\phi_k^{[1]}$ or $v^{[1]}$, but to find differential equations for A_n and B_n which can be obtained by avoiding secular terms in the order ε solution $\phi_k^{[1]}(t_0,t_1)$. So, we just need to look for any resonant terms in $\hat{p}_k$, i.e., for terms which are solutions of the homogeneous equation. Setting all coefficients of the resonant terms equal to zero, gives us

$$\begin{aligned}\frac{dA_k}{dt_1} = \frac{\lambda\pi^2}{2}\Bigg[&4k^2\left(B_{2k}B_k + A_{2k}A_k\right) + \sum_{n<k} n\Big(B_n\left((n+k)B_{n+k} + (k-n)B_{k-n}\right)\\ &+A_n\left((n+k)A_{n+k} - (k-n)A_{k-n}\right)\Big) + \sum_{n>k} n\Big(B_n\left((n+k)B_{n+k} + (n-k)B_{n-k}\right)\\ &+A_n\left((n+k)A_{n+k} + (n-k)A_{n-k}\right)\Big)\Bigg],\end{aligned} \tag{19a}$$

$$\begin{aligned}\frac{dB_k}{dt_1} = \frac{\lambda\pi^2}{2}\Bigg[&4k^2\left(A_kB_{2k} - B_kA_{2k}\right) + \sum_{n<k} n\Big(A_n\left((n+k)B_{n+k} - (k-n)B_{k-n}\right)\\ &- B_n\left((n+k)A_{n+k} + (k-n)A_{k-n}\right)\Big) + \sum_{n>k} n\Big(A_n\left((n+k)B_{n+k} - (n-k)B_{n-k}\right)\\ &-B_n\left((n+k)A_{n+k} - (n-k)A_{n-k}\right)\Big)\Bigg].\end{aligned} \tag{19b}$$

It is clear that the equation for A_k and B_k are coupled to the equations for A_j and B_j for $j = 2k, n+k, n-k$, and n. Thus, the system consisting of (19a)–(19b) for all values of k is an infinite-dimensional coupled system of differential equation, which usually cannot be solved explicitly. Furthermore, the coupling terms are such that the system cannot be truncated to a finite dimensional one. Sometimes indirect approaches such as characteristic coordinates might help. Characteristic coordinates can produce somewhat simpler equations to describe the dynamics of a nonlinear wave problem, as shown by Darmawijoyo et al. [14] and also Malookani et al. [13].

If we compare the results obtained so far with previous work of Mandal and Wahi [8], then it should be observed that in [8], it is directly assumed that the solution is a combination of a stationary and a time-dependent part, without introducing proper perturbation expansions or a mathematical derivation. The assumed form of the solution is a truncated Fourier series and is substituted into the PDE to obtain the modal interaction. Because truncation is done initially, a lot of modal interactions are neglected in [8]. In comparison, we rather apply a more analytic approach and multiple time-scales, as we have shown in the previous sections. By using perturbation expansions and multiple-time scales, we arrive at an ODE system (19a)–(19b) which represents the interactions between all wave modes in the $\mathcal{O}(1)$-part of the approximations of the solution of the problem.

4.3. Characteristic coordinates

In this section we will use another approach to simplify and to solve the problem. A combination method based on characteristic coordinates and multiple time-scales will be used. We define $\xi = x - t_0$ and $\eta = x - t_0$. By introducing characteristic coordinates, we have to extend our problem domain to the whole real line by introducing odd and 2-periodic function extensions in x.

We consider again the problem formulations in its Dirichlet form (17a)–(17d). To make every term of $\tilde{p}$ odd and 2-periodic in x, we only have to extend $(1-x)$ by using its Fourier sine series. Then, the function $\tilde{p}$ becomes

$$\tilde{p}(x,t_0) = \lambda\left[2\tilde{v}_x^{[0]}(0,t_0)\tilde{v}_{t_0t_0}^{[0]} + R(x)\left[2\tilde{v}_{xt_0}^{[0]}(0,t_0)\tilde{v}_{xt_0}^{[0]} + \tilde{v}_{xt_0t_0}^{[0]}(0,t)\tilde{v}_x^{[0]}\right]\right], \tag{20}$$

where

$$R(x) = \sum_{n=1}^{\infty} \frac{2\sin(n\pi x)}{n\pi}.$$

The problem domain is now extended to the whole real line while preserving its validity in the original domain $[0,1]$, including satisfying the BCs. We set $\tilde{v}(x,t_0,t_1) = w(\xi,\eta,t_1)$. To avoid too many recomputations, we also define the perturbation expansion for w, as:

$$w = w^{[0]} + \varepsilon w^{[1]} + \mathcal{O}(\varepsilon^2),$$

where $v^{[0]} = w^{[0]}$ and $v^{[1]} = w^{[1]}$. Thus, we have the following problems

$$\mathcal{O}(1): \quad 4w^{[0]}_{\xi\eta} = 0, \tag{21a}$$
$$w^{[0]}(\xi,\xi,0) = f(\xi), \tag{21b}$$
$$-\, w^{[0]}_{\xi}(\xi,\xi,0) + w^{[0]}_{\eta}(\xi,\xi,0) = g(\xi), \tag{21c}$$
$$\mathcal{O}(\varepsilon): \quad 4w^{[1]}_{\xi\eta} = 2w^{[0]}_{\eta t_1} - 2w^{[0]}_{\xi t_1} + P(\xi,\eta,t_1), \tag{21d}$$
$$w^{[1]}(\xi,\xi,0) = 0, \tag{21e}$$
$$-\, w^{[1]}_{\xi}(\xi,\xi,0) + w^{[1]}_{\eta}(\xi,\xi,0) = -w^{[0]}_{t_1}(\xi,\xi,0), \tag{21f}$$

where $P(\xi,\eta,t_1) = \bar{p}(x,t_0,t_1)$. The $\mathcal{O}(1)$-problem can easily be solved, yielding

$$w^{[0]}(\xi,\eta,t_1) = \varphi(\xi,t_1) + \psi(\eta,t_1),$$

where φ and ψ are arbitrary function in t_1 satisfying

$$\varphi(\xi,0) = \frac{1}{2}\left(f(\xi) - \int_{\xi_0}^{\xi} g(z)dz\right), \qquad \psi(\eta,0) = \frac{1}{2}\left(f(\eta) + \int_{\eta_0}^{\eta} g(z)dz\right). \tag{22}$$

Moreover, φ and ψ, and also their derivatives are 2-periodic in their first arguments. The functions φ and ψ can be obtained completely by removing secular terms in the $\mathcal{O}(\varepsilon)$-problem. The detailed computations are presented in Appendix A, where it is shown that φ and ψ can be obtained by solving the following system of PDEs:

$$\varphi_{t_1}(\xi,t_1) = \frac{\lambda}{2}\left(\varphi^2_{\xi}(\xi,t_1) - \int_0^1 [\varphi_{\zeta\zeta}(\zeta,t_1) + \varphi_{\zeta\zeta}(\zeta+1,t_1)]\varphi(2\zeta-\xi,t_1)d\zeta\right), \tag{23a}$$

$$\psi_{t_1}(\eta,t_1) = -\frac{\lambda}{2}\left(\psi^2_{\eta}(\eta,t_1) - \int_0^1 [\psi_{\zeta\zeta}(\zeta,t_1) + \psi_{\zeta\zeta}(\zeta+1,t_1)]\psi(2\zeta-\eta,t_1)d\zeta\right). \tag{23b}$$

Because the exact solution of this system may not be available, we will apply a numerical method in the next section to obtain φ and ψ from (23a)–(23b).

5. Numerical integration

5.1. Characteristic system

To compute the functions φ and ψ from (23a)–(23b) numerically, we apply a Lax–Wendroff method for which the detailed scheme is derived and can be found in Appendix B.1. We set the domain for $\tilde{v}^{[1]}$ as follows

$$D_{\varphi} = [-1,1]\times[0,1], \quad D_{\psi} = [0,2]\times[0,1].$$

For the initial conditions, we take $f(x) = \delta\sin(\pi x)$, where δ is some constant, and $g(x) = 0$. It should be noted that the quadratic terms in both φ and ψ in (23a)–(23b) may cause difficulties in achieving numerical stability. We overcome these difficulties by having a trial-and-error search for many combinations of the constants involved to obtain stable results. The influencing constants include c, b, δ, Δt_1, and $\Delta\xi$.

It turned out that the values of λ and δ influence the stability highly. The coefficient λ itself depends on two problem-defined constants c and b. Smaller λ and δ values give better stability results. Firstly, we set $\delta = 0.4$, $b = 0.05$, and $c = 0$. For the discretization setup, we use $\Delta\xi = \Delta\eta = 0.02$ and $\Delta t_1 = 0.001$. The results can be seen as time snapshots in Fig. 3 and as a map in Fig. 4.

5.2. Numerical results for different values of c

The value of c determines the type of boundary condition at $x = 0$ as has been explained in Section 3.3. Considering this observation, we compute the numerical approximations of the solutions of (23a)–(23b) for different values of c (and b). As we have computed these approximations for the Dirichlet-case in the previous subsection, we will consider two other cases, i.e., the Robin condition with $c = -0.2$ and $b = 0.5$, and the Neumann condition with $c = 0.5$ and $b = 0.75$. The resulting solution maps for these

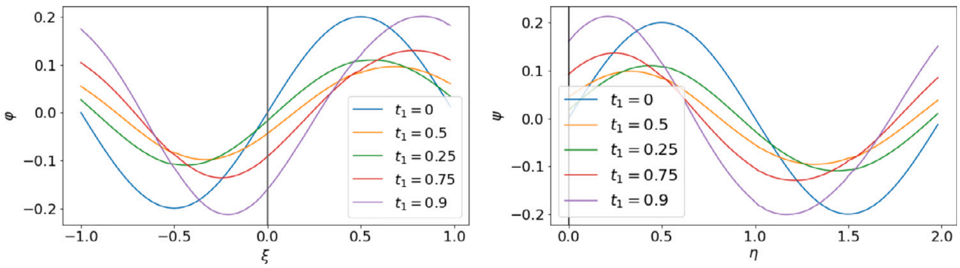

Fig. 3. Numerical plots of the functions φ and ψ as solutions of (23a)–(23b) for $t_1 = 0, 0.25, \dots, 0.9$.

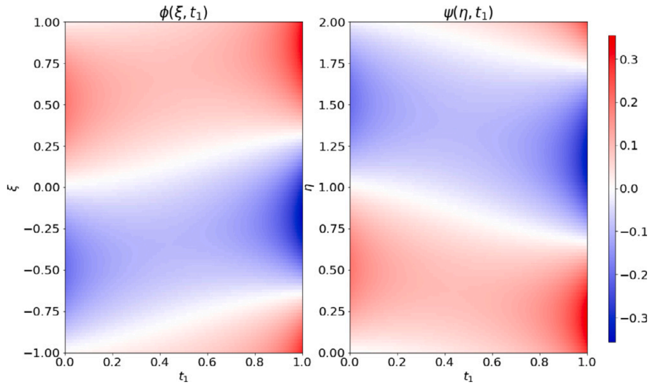

Fig. 4. Numerical plots of the functions φ and ψ as solutions of (23a)–(23b).

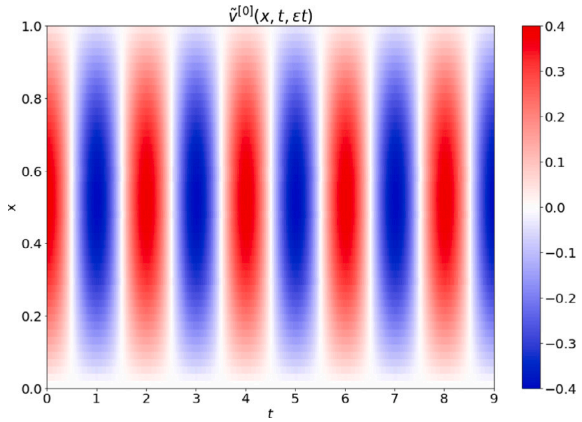

Fig. 5. Numerical approximations (based on (23a)–(23b)) of the solution v in the Dirichlet case.

cases are shown in Figs. 5–7, respectively. We can see how the solution at the boundary point $x = 0$ is changing for different values of c.

Observe that in the Robin and in the Neumann case, the profile of the initial wave does not correspond to the initial condition $f(x)$, which should have for instance the value 0 at $x = 0$. This is due to the correction done directly by the first iteration in the numerical scheme to make sure every boundary condition is met. To satisfy all boundary conditions correctly, the initial wave profile then is corrected accordingly.

5.3. Comparison of results

We will compare the numerical results for the characteristic system (23a)–(23b) with numerical results for the original system (3a)–(3d). A detailed derivation of the numerical scheme can be found in Appendix B.2. For further comparison, we also simulate the analytical approximation which is obtained from the straightforward perturbation expansion (14). We plot some snapshots

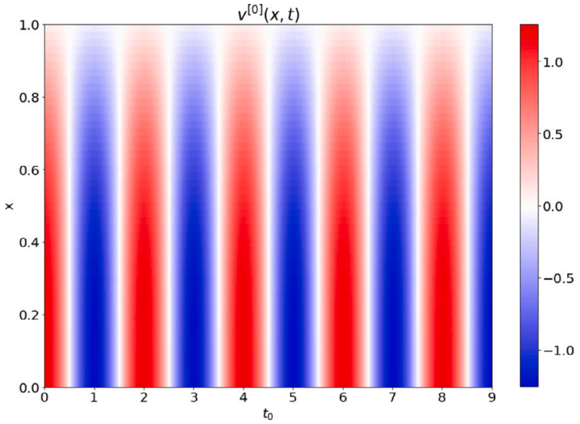

Fig. 6. Numerical approximations (based on (23a)–(23b)) of the solution v in the Neumann case.

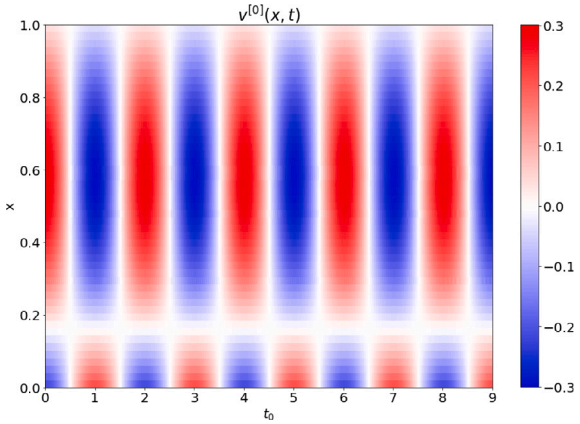

Fig. 7. Numerical approximations (based on (23a)–(23b)) of the solution v in the Robin case.

of the wave profiles computed by using different approaches at some fixed times. We compare 3 approaches, i.e., the analytical approximation (Eq. (14)), the numerical approximation of the characteristic system (23a)–(23b), and the numerical approximation of the original system (3a)–(3d). In these computations, we use $\varepsilon = 0.1$, $c = -0.3$ and $b = 0.5$ for the Robin case; $c = 0$ and $b = 0.3$ for the Dirichlet case; and lastly, $c = 0.5$ and $b = 0.75$ for the Neumann case. The plots for each case are shown in Figs. 8–10. The behavior of the map in Fig. 7 around $x \approx 0.18$ may seem strange for the Robin condition, where it always has value 0 around $x \approx 0.18$. This is due to the fact that v is not the only time-dependent part in terms of the original domain. In the original coordinates (see Fig. 10), this abnormality does not occur anymore. All approximations are computed up to $t = 9$. So, the approximations are all close to each other. For longer t values, only the approximations of the characteristic system and the numerical approximations of the original system turn out to remain close.

6. Conclusion

In this paper, a detailed description and validation are given on how to construct approximation of solutions for a vibrating string problem, where the string is in contact with an obstacle at one of its ends. Perturbation methods as well as numerical methods are used to construct accurate approximations of the solutions of the problem. It is shown how a nonlinear boundary value problem on a fixed interval can be obtained for a rather general, but smooth shape of the obstacle. For a specific case with a parabolic-shaped obstacle, it is explicitly shown in diagrams what kind of simplified boundary conditions at the obstacle attachment–detachment point are obtained in the parameter space. By using characteristic coordinates, a two time-scales perturbation method, and a Lax–Wendroff numerical method, the dynamics of the string is successfully analyzed and simulated. The applicability of the presented approach opens possibilities for future research on even more complicated constrained string problems.

The presented approach opens also the possibility to determine which frequencies become more (or less) important in time. By using the fast-Fourier-transform to the obtained approximations in characteristic coordinates, the approximation at fixed times can be decomposed into (amplitude of) oscillation modes and their corresponding frequencies. In this was the change in sound of musical instrument can be studied (see [12]).

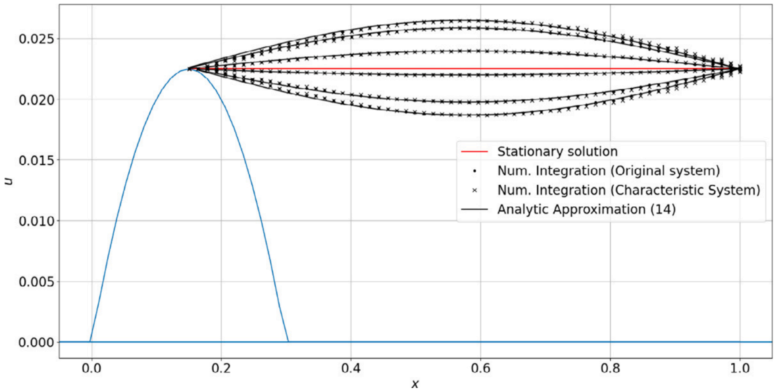

Fig. 8. Standing wave profile snapshots in the Dirichlet case.

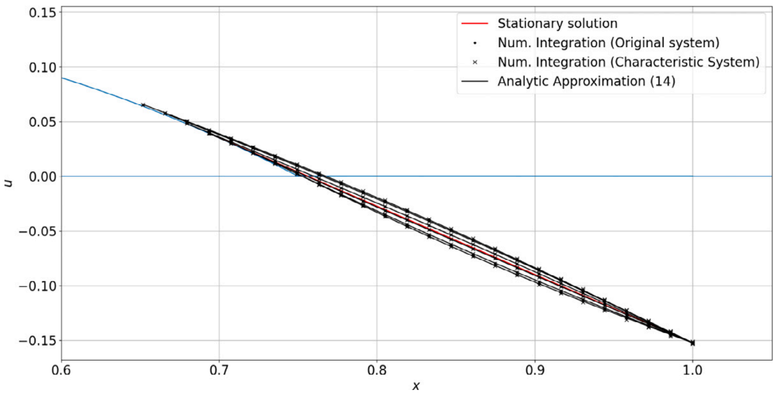

Fig. 9. Standing wave profile snapshots in the Neumann case.

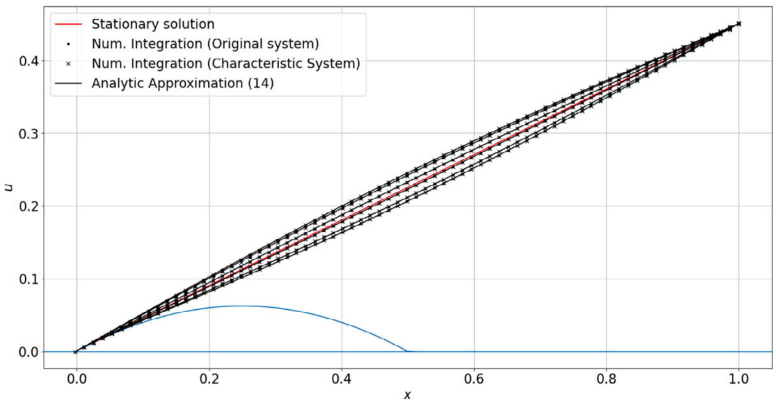

Fig. 10. Standing wave profile snapshots in the Robin case.

CRediT authorship contribution statement

A.F. Ihsan: Formal analysis, Investigation, Writing – original draft. **W.T. van Horssen:** Conceptualization, Formal analysis, Investigation, Supervision. **J.M. Tuwankotta:** Formal analysis, Methodology, Supervision, Writing – review & editing.

Declaration of competing interest

The authors declare that they have no known competing financial interests or personal relationships that could have appeared to influence the work reported in this paper.

Data availability

No data was used for the research described in the article.

Appendix A. Computing the characteristic system

In this appendix, a detailed derivation of the characteristic system will be presented. Consider the $\mathcal{O}(\varepsilon)$-problem (21d)–(21f). We want to recognize and to remove the unbounded (or secular) terms in the solution. We integrate first the $\mathcal{O}(\varepsilon)$-problem with respect to η and obtain

$$\int_{\xi}^{\eta} 4w^{[1]}_{\xi\bar{\eta}}(\xi,\bar{\eta},t_1)d\bar{\eta} = 2\int_{\xi}^{\eta}\left(w^{[0]}_{\bar{\eta}t_1} - w^{[0]}_{\xi t_1}\right)d\bar{\eta} + \int_{\xi}^{\eta} P(\xi,\bar{\eta},t_1)d\bar{\eta}. \tag{A.1}$$

In order to detect any secular terms, we need to look at $P(\xi,\eta,t_1)$ explicitly in terms of characteristic coordinates. For that matter, we rewrite (20) as follows

$$\tilde{p}(x,t_0,t_1) = \lambda\left[2G_s(x,t_0,t_1) + F_s(x,t_0,t_1)\right], \tag{A.2}$$

where $G_s = \tilde{v}^{[0]}_x(0,t_0,t_1)\tilde{v}^{[0]}_{t_0t_0}$, and $F_s(x,t_0,t_1) = R(x)\left[2\tilde{v}^{[0]}_{xt}(0,t_0,t_1)\tilde{v}^{[0]}_{xt} + \tilde{v}^{[0]}_{xtt}(0,t_0,t_1)\tilde{v}^{[0]}_x\right]$. In characteristic coordinates, G_s can be written as $G_s = (\psi_{\eta\eta} + \varphi_{\xi\xi})\bar{G}_s$, where

$$\bar{G}_s(\xi,\eta,t_1) = \sum_{n=1}^{\infty} n\pi\left[A_n\sin\left(\frac{n\pi(\eta-\xi)}{2}\right) + B_n\cos\left(\frac{n\pi(\eta-\xi)}{2}\right)\right].$$

For the integration with respect to η it should be observed that the term $\varphi_{\xi\xi}\bar{G}_s$ in G_s does not lead to unbounded terms, and so

$$G_s = \psi_{\eta\eta}\bar{G}_s + n.s.t.,$$

where $n.s.t.$ stands for *non-secular terms*. For F_s, we will separate the terms in secular and nonsecular terms in the following way. Recall from (18) that we have $\tilde{v}^{[0]}(x,t_0,t_1) = \sum_{n=1}^{\infty}\phi_n(t_0,t_1)\sin(n\pi x)$. Observe then that

$$R(x)\tilde{v}^{[0]}_{xt_0}(0,t_0,t_1)\tilde{v}^{[0]}_{xt_0} = 2\sum_{k=1}^{\infty}\sum_{n=1}^{\infty}\sum_{m=1}^{\infty}\frac{mn}{k}\pi\sin(k\pi x)\cos(n\pi x)\frac{\partial\phi_m}{\partial t_0}\frac{\partial\phi_n}{\partial t_0},$$

$$R(x)\tilde{v}^{[0]}_{xt_0t_0}(0,t_0,t_1)\tilde{v}^{[0]}_x = -2\sum_{k=1}^{\infty}\sum_{n=1}^{\infty}\sum_{m=1}^{\infty}\frac{m^3n}{k}\pi^3\sin(k\pi x)\cos(n\pi x)(\phi_m)(\phi_n),$$

which can be combined to

$$F_s(x,t_0,t_1) = 2\sum_{n=1}^{\infty}\sum_{m=1}^{\infty}\sum_{k=1}^{\infty}\frac{mn}{k}\pi\sin(k\pi x)\cos(n\pi x)\left[2\frac{\partial\phi_m}{\partial t_0}\frac{\partial\phi_n}{\partial t_0} - (m\pi)^2(\phi_m)(\phi_n)\right].$$

Terms in the above equation will lead to secular terms in $w^{[1]}$ only if $k=m$, $k=\pm(2n-m)$ or $k=2n+m$. Separating these terms, we obtain $F_s = 2F(x,t_0,t_1) + n.s.t$, where

$$\begin{aligned} F(x,t_0,t_1) = \frac{\pi}{2}\sum_{n=1}^{\infty}\sum_{m=1}^{\infty} mn\Bigg[&\frac{\sin((m+3n)\pi x)+\sin((m+n)\pi x)}{2n+m} \\ &-\frac{\sin((m-3n)\pi x)+\sin((m-n)\pi x)}{2n-m} \\ &+\frac{\sin((m+n)\pi x)+\sin((m-n)\pi x)}{m}\Bigg]\left[2\frac{\partial\phi_m}{\partial t_0}\frac{\partial\phi_n}{\partial t_0} - (m\pi)^2(\phi_m)(\phi_n)\right].\end{aligned}$$

So, in terms of characteristic coordinates, Eq. (A.2) above becomes

$$P(\xi,\eta,t_1) = 2\lambda\left[\psi_{\eta\eta}\bar{G}_s + \bar{F}\right] + n.s.t.,$$

where $\bar{F}(\xi,\eta,t_1) = F(x,t_0,t_1)$. Integration of Eq. (A.1) leads to

$$2\left|w^{[1]}_{\xi}(\xi,\bar{\eta},t_1)\right|_{\xi}^{\eta} = \int_{\xi}^{\eta}\psi_{\bar{\eta}t_1}d\bar{\eta} - (\eta-\xi)\varphi_{\xi t_1} + \lambda\left[\int_{\xi}^{\eta}\psi_{\bar{\eta}\bar{\eta}}\bar{G}_s d\bar{\eta} + \int_{\xi}^{\eta}\bar{F}\ d\bar{\eta} + n.s.t.\right]. \tag{A.3}$$

To find the secular terms, we look for terms that are linear in $t = \frac{\eta-\xi}{2}$. To check the integrals inside the square brackets, we will use the Fourier series for φ and ψ. From (18), we derive that

$$\varphi(\xi,t_1) = \frac{1}{2}\sum_{n=1}^{\infty}(A_n\cos(n\pi\xi) + B_n\sin(n\pi\xi)),$$

$$\psi(\eta,t_1)=\frac{1}{2}\sum_{n=1}^{\infty}(-A_n\cos(n\pi\eta)+B_n\sin(n\pi\eta)).$$

We then see that

$$\bar{G}_s\psi_{\eta\eta}=-\frac{1}{2}\sum_{n=1}^{\infty}\sum_{m=1}^{\infty}mn^2\pi^3\left[A_m\sin\left(\frac{m\pi(\eta-\xi)}{2}\right)+B_m\cos\left(\frac{m\pi(\eta-\xi)}{2}\right)\right]$$
$$\left[-A_n\cos(n\pi\eta)+B_n\sin(n\pi\eta)\right].$$

Observe that terms for which $m\neq 2n$, are not secular. Thus, we separate the terms in $\bar{G}_s\psi_{\eta\eta}=\bar{G}+n.s.t.$, where

$$\bar{G}=-\sum_{n=1}^{\infty}(n\pi)^3(A_{2n}\sin(n\pi(\eta-\xi))+B_{2n}\cos(n\pi(\eta-\xi)))(-A_n\cos(n\pi\eta)+B_n\sin(n\pi\eta)).$$

The integrals of $\bar{F}$ and $\bar{G}$ become secular terms when the integral over its periodic interval does not vanish. Thus, we split this term as follows

$$\int_{\xi}^{\eta}\bar{F}\,d\bar{\eta}=\int_{\xi}^{\eta}\left[\bar{F}-\frac{1}{2}\int_0^2\bar{F}\,d\zeta\right]d\bar{\eta}+\frac{\eta-\xi}{2}\int_0^2\bar{F}\,d\zeta.$$

We apply a similar step to the integral of $\bar{G}$. Setting all secular terms to zero, we obtain

$$\varphi_{\xi t_1}=\frac{\lambda}{2}\int_0^2[\bar{F}(\xi,\zeta,t_1)+\bar{G}(\xi,\zeta,t_1)]d\zeta. \tag{A.4}$$

By computing the integrals, the PDE (A.4) in Fourier series form becomes

$$\begin{aligned}\varphi_{\xi t_1}=&-\frac{\lambda\pi^3}{2}\sum_{n=1}^{\infty}n\Bigg\{n^2[(A_{2n}A_n+B_{2n}B_n)\sin(n\pi\xi)+(A_{2n}B_n-B_{2n}A_n)\cos(n\pi\xi)]\\&+\sum_{m=1}^{\infty}\frac{m}{2}\Big[(m+n)[(B_mB_n-A_mA_n)\sin((m+n)\pi\xi)+(A_mB_n+A_nB_m)\cos((m+n)\pi\xi)]\\&+(m-n)[(A_mB_n-A_nB_m)\cos((m-n)\pi\xi)+(A_mA_n+B_mB_n)\sin((m-n)\pi\xi)]\Big]\Bigg\}.\end{aligned} \tag{A.5}$$

Similarly, the PDE for ψ can be obtained by integrating (A.3) with respect to ξ, i.e.

$$\begin{aligned}\psi_{\eta t_1}=&\frac{\lambda\pi^3}{2}\sum_{n=1}^{\infty}n\Bigg\{n^2[(A_{2n}A_n+B_{2n}B_n)\sin(n\pi\eta)-(A_{2n}B_n-B_{2n}A_n)\cos(n\pi\eta)]\\&+\sum_{m=1}^{\infty}\frac{m}{2}\Big[(m+n)[(B_mB_n-A_mA_n)\sin((m+n)\pi\eta)-(A_mB_n+A_nB_m)\cos((m+n)\pi\eta)]\\&+(m-n)[(A_mA_n+B_mB_n)\sin((m-n)\pi\eta)-(A_mB_n-A_nB_m)\cos((m-n)\pi\eta)]\Big]\Bigg\}.\end{aligned} \tag{A.6}$$

The PDE (A.5) or (A.6) obtained by removing secular terms using characteristic coordinates should be equivalent to the infinite-dimensional coupled system (19a) and (19b). By multiplying both sides of (A.5) with $\sin(k\pi\xi)$ and by integrating with respect to ξ over the interval $[0,2]$, we will obtain the same equation as (19a). Similarly, we multiply again (A.5) with $\cos(k\pi\xi)$ and integrate from $\xi=0$ to $\xi=2$. The result is (19b). Our goal is to find a solution in terms of characteristic coordinates. To do so, we have to obtain a system of PDEs that only involve φ and ψ. We actually can use directly the secular terms from Eq. (A.3) or (A.4). Observe again that these terms are

$$\begin{aligned}\varphi_{\xi t_1}=&\frac{\lambda}{2}\int_0^2\Bigg[\psi_{\bar{\eta}\bar{\eta}}\left[\varphi_{\xi}+\psi_{\bar{\eta}}\right]_{\xi=-\eta}+\sum_{n=1}^{\infty}\frac{1}{n\pi}\sin\left(\frac{n\pi(\xi+\bar{\eta})}{2}\right)\Big[2\psi_{\bar{\eta}\bar{\eta}}\left[-\phi_{\xi\xi}+\psi_{\bar{\eta}\bar{\eta}}\right]_{\xi=-\eta}\\&+\psi_{\bar{\eta}}\left[\phi_{\xi\xi\xi}+\psi_{\bar{\eta}\bar{\eta}\bar{\eta}}\right]_{\xi=-\eta}\Big]\Bigg]d\bar{\eta}.\end{aligned}$$

To simplify the PDE for φ further, we integrate (A.5) with respect to ξ and obtain

$$\begin{aligned}\varphi_{t_1}=&K_1(t_1)+\frac{\lambda\pi^2}{2}\sum_{n=1}^{\infty}n\Bigg\{n(A_{2n}A_n+B_{2n}B_n)\cos(n\pi\xi)-(A_{2n}B_n-B_{2n}A_n)\sin(n\pi\xi)\\&+\sum_{m=1}^{\infty}\frac{m}{2}\Big[(B_mB_n-A_mA_n)\cos((m+n)\pi\xi)-(A_mB_n+A_nB_m)\sin((m+n)\pi\xi)\\&-(A_mB_n-A_nB_m)\sin((m-n)\pi\xi)+(A_mA_n+B_mB_n)\cos((m-n)\pi\xi)\Big]\Bigg\},\end{aligned} \tag{A.7}$$

for some function $K_1(t_1)$. Observe that the second series in (A.7) can be reduced to

$$\frac{nm\pi^2}{2}\sum_{n=1}^{\infty}\sum_{m=1}^{\infty}(A_n\sin(n\pi\xi)-B_n\cos(n\pi\xi))(A_m\sin(m\pi\xi)-B_m\cos(m\pi\xi))$$
$$=\frac{1}{2}\left(n\pi\sum_{n=1}^{\infty}(-A_n\sin(n\pi\xi)+B_n\cos(n\pi\xi))\right)^2=\frac{1}{2}\varphi_\xi^2(\xi,t_1).$$

Every series in the form $\sum_{n=1}^{\infty}a_n\cos(n\pi x)+b_n\sin(n\pi x)$ can be rewritten in $\sum_{n=-\infty}^{\infty}c_n\exp(in\pi x)$, where $c_n=\frac{1}{2}(a_n-ib_n)$ and $c_{-n}=\overline{c_n}$. Using this exponential form of the Fourier series, the first series in Eq. (A.5) becomes $\frac{\pi^2}{2}\sum_{n\in\mathbb{Z}}n^2C_ne^{in\pi\xi}$, where $C_n=\frac{1}{2}[(A_{2n}A_n+B_{2n}B_n)+i(A_{2n}B_n-B_{2n}A_n)]=\frac{1}{2}(A_{2n}-iB_{2n})(A_n+iB_n)$.

We will use the convolution theorem to factorize the first series in (A.7). We rewrite first φ and ψ in exponential form, i.e., $\varphi(\xi,t_1)=\sum_{n\in\mathbb{Z}}\hat{\varphi}_ne^{in\pi\xi}$ and $\psi(\eta,t_1)=\sum_{n\in\mathbb{Z}}\hat{\psi}_ne^{in\pi\xi}$, where $\hat{\varphi}_n=\frac{1}{4}(A_n-iB_n)$ and $\hat{\psi}_n=\frac{1}{4}(A_n+iB_n)$. Next, denoting $P(\xi,t_1)=\varphi_{\xi\xi}\left(\frac{\xi}{2},t_1\right)+\varphi_{\xi\xi}\left(\frac{\xi+2}{2},t_1\right)$, we find $P(\xi)=\sum_{n\in\mathbb{Z}}\hat{P}_ne^{in\pi\xi}$, where $\hat{P}_n=\frac{1}{2}n^2\pi^2(A_{2n}-iB_{2n})$. We then obtain

$$\frac{1}{2}n^2\pi^2C_n=\frac{1}{4}n^2\pi^2(A_{2n}-iB_{2n})(A_n+iB_n)=\frac{1}{2}\hat{P}_n\hat{\psi}_n.$$

Now, we can apply the convolution theorem in the following way:

$$\frac{\pi^2}{2}\sum_{n\in\mathbb{Z}}n^2C_ne^{in\pi\xi}=\frac{1}{4}\sum_{n\in\mathbb{Z}}2\hat{P}_n\hat{\psi}_ne^{in\pi\xi}=\frac{1}{4}(P*\psi)(\xi)$$
$$=\frac{1}{4}\int_0^2\left[\varphi_{\zeta\zeta}\left(\frac{\zeta}{2},t_1\right)+\varphi_{\zeta\zeta}\left(\frac{\zeta+2}{2},t_1\right)\right]\psi(\xi-\zeta,t_1)d\zeta$$
$$=\frac{1}{2}\int_0^1[\varphi_{\zeta\zeta}(\zeta,t_1)+\varphi_{\zeta\zeta}(\zeta+1,t_1)]\psi(\xi-2\zeta,t_1)d\zeta.$$

Wrapping up, we obtain

$$\varphi_{t_1}(\xi,t_1)=K_1(t_1)+\frac{\lambda}{2}\left(\varphi_\xi^2(\xi,t_1)+\int_0^1[\varphi_{\zeta\zeta}(\zeta,t_1)+\varphi_{\zeta\zeta}(\zeta+1,t_1)]\psi(\xi-2\zeta,t_1)d\zeta\right).\tag{A.8a}$$

Applying the same procedure to (A.6) yields a similar equation for ψ, i.e.,

$$\psi_{t_1}(\eta,t_1)=K_2(t_1)-\frac{\lambda}{2}\left(\psi_\eta^2(\eta,t_1)+\int_0^1[\psi_{\zeta\zeta}(\zeta,t_1)-\psi_{\zeta\zeta}(\zeta+1,t_1)]\varphi(\eta-2\zeta,t_1)d\zeta\right).\tag{A.8b}$$

We can see that the PDEs for φ and ψ are similar to transport equations with opposing directions. The differences here are that we have a quadratic advection term and an additional, coupled convolution term. Odd symmetry of φ and ψ, i.e. $\varphi(a,t_1)=-\psi(-a,t_1)$, can be used to decouple the PDEs (A.8a) and (A.8b), so that

$$\varphi_{t_1}(\xi,t_1)=K_1(t_1)+\frac{\lambda}{2}\left(\varphi_\xi^2(\xi,t_1)-\int_0^1[\varphi_{\zeta\zeta}(\zeta,t_1)+\varphi_{\zeta\zeta}(\zeta+1,t_1)]\varphi(2\zeta-\xi,t_1)d\zeta\right),\tag{A.9a}$$

$$\psi_{t_1}(\eta,t_1)=K_2(t_1)-\frac{\lambda}{2}\left(\psi_\eta^2(\eta,t_1)-\int_0^1[\psi_{\zeta\zeta}(\zeta,t_1)+\psi_{\zeta\zeta}(\zeta+1,t_1)]\psi(2\zeta-\eta,t_1)d\zeta\right).\tag{A.9b}$$

To compute K_1 and K_2, we can use the periodicity properties of φ and ψ. Observe that computing (A.9a) at $\xi=a$ for arbitrary $a\in(0,1)$ yields

$$-\psi_{t_1}(-a,t_1)=K_1+\frac{\lambda}{2}\left(\psi_\eta^2(-a,t_1)-\int_0^1[\psi_{\zeta\zeta}(\zeta+1,t_1)+\psi_{\zeta\zeta}(\zeta,t_1)]\psi(a+2\zeta,t_1)d\zeta\right).\tag{A.10a}$$

On the other hand, computing (A.9b) at $\eta=-a$ gives us

$$\psi_{t_1}(-a,t_1)=K_2-\frac{\lambda}{2}\left(\psi_\eta^2(-1,t_1)-\int_0^1[\psi_{\zeta\zeta}(\zeta,t_1)+\psi_{\zeta\zeta}(\zeta+1,t_1)]\psi(2\zeta+a,t_1)d\zeta\right).\tag{A.10b}$$

Adding up (A.10a) and (A.10b) gives us $K_1+K_2=0$ or equivalently $K_1(t_1)=-K_2(t_1)$. We can assign to K_1 any arbitrary function of t_1 since in the function $w^{[0]}$ it will not play any role ($K_1+K_2=0$). For convenience, we will set $K_1=0$, and so we obtain system (23a)–(23b)

To check the correctness of this derivation, we resubstitute

$$\varphi(\xi,t_1)=\frac{1}{2}\sum_{n=1}^{\infty}(A_n\cos(n\pi\xi)+B_n\sin(n\pi\xi)),$$

into (A.9a). The second term of (A.9a) directly yields the second series of (A.7). For the third term, we compute

$$-\frac{1}{2}\int_{-1}^{0}[\varphi_{\zeta\zeta}(\zeta,t_1)+\varphi_{\zeta\zeta}(\zeta+1,t_1)]\varphi(2\zeta-\xi,t_1)d\zeta$$

$$= \frac{n^2\pi^2}{2}\sum_{n=1}^{\infty}((A_{2n}A_n + B_{2n}B_n)\cos(n\pi\xi) - (A_{2n}B_n - A_nB_{2n})\sin(n\pi\xi)),$$

which equals to the first series in (A.7). Thus, Eq. (A.9a) is equivalent with (A.7). Further derivation with respect to ξ gives us (A.5). Applying the Galerkin projection as has done in Section 4.2 leads again to system (19a)–(19b).

Appendix B. Setup of the numerical scheme

B.1. The Lax–Wendroff method for the characteristic system (23a)–(23b)

In this section we will describe the numerical scheme to be applied to system (23a)–(23b). To construct this scheme, we expand first φ in a second order Taylor series around t_1, so that

$$\varphi(\xi, t_1 + \Delta t_1) = \varphi(\xi, t_1) + \Delta t_1\varphi_{t_1}(\xi, t_1) + \frac{(\Delta t_1)^2}{2}\varphi_{t_1t_1}(\xi, t_1) + \mathcal{O}((\Delta t_1)^3). \tag{B.1}$$

Let

$$\Phi(\xi, t_1) = \int_0^1 [\varphi_{\zeta\zeta}(\zeta, t_1) + \varphi_{\zeta\zeta}(\zeta + 1, t_1)]\varphi(2\zeta - \xi, t_1)d\zeta.$$

From (23a), we then obtain

$$\varphi_{t_1t_1}(\xi, t_1) = \frac{\lambda}{2}\left(\lambda(2\varphi_\xi^2\varphi_{\xi\xi} - \varphi_\xi\Phi_\xi) - \Phi_{t_1}\right), \tag{B.2}$$

where

$$\begin{aligned}\Phi_\xi &= \int_0^1 [\varphi_{\zeta\zeta}(\zeta, t_1) + \varphi_{\zeta\zeta}(\zeta + 1, t_1)]\varphi_\xi(2\zeta - \xi, t_1)d\zeta,\\ \Phi_{t_1} &= \int_0^1 \Big\{[\varphi_{\zeta\zeta t_1}(\zeta, t_1) + \varphi_{\zeta\zeta t_1}(\zeta + 1, t_1)]\varphi(2\zeta - \xi, t_1)\\ &\quad + [\varphi_{\zeta\zeta}(\zeta, t_1) + \varphi_{\zeta\zeta}(\zeta + 1, t_1)]\varphi_{t_1}(2\zeta - \xi, t_1)\Big\}d\zeta.\end{aligned}$$

Substituting (23a) and (B.2) into (B.1) yields

$$\begin{aligned}\varphi(\xi, t_1 + \Delta t_1) &= \varphi(\xi, t_1) + \frac{\Delta t_1\lambda}{2}\left(\varphi_\xi^2(\xi, t_1) - \Phi(\xi, t_1)\right)\\ &\quad + \frac{\lambda(\Delta t_1)^2}{4}\left(\lambda(\varphi_\xi^2\varphi_{\xi\xi} - \varphi_\xi\Phi_\xi) - \Phi_{t_1}\right) + \mathcal{O}((\Delta t_1)^3).\end{aligned} \tag{B.3}$$

We solve (23a) for φ numerically in a domain $D_\varphi = [\xi_{min}, \xi_{max}] \times [0, T_1]$. Let Δt_1 and $\Delta\xi$ be lengths of small interval slices in t_1 and ξ direction. We construct a discrete domain of size $N_\xi \times N_{t_1}$, which divides the real domain into finite countable grids with size $\Delta\xi \times \Delta t_1$ where $\Delta\xi = \frac{\xi_{max} - \xi_{min}}{N_\xi}$ and $\Delta t_1 = \frac{T_1}{N_{t_1}}$. Using this discretization, we denote $\varphi_i^n = \varphi(\xi_{min} + i\Delta\xi, n\Delta t_1)$. To discretize (B.3), we use the following forward time and center space derivative approximations:

$$\varphi_{t_1} \approx \frac{\varphi_i^{n+1} - \varphi_i^n}{\Delta t_1}, \quad \varphi_\xi \approx \frac{\varphi_{i+1}^n - \varphi_{i-1}^n}{2\Delta\xi}, \quad \varphi_{\xi\xi} \approx \frac{\varphi_{i+1}^n - 2\varphi_i^n + \varphi_{i-1}^n}{(\Delta\xi)^2}.$$

For the convolution integral, we use the following Riemann sum:

$$\int_a^b F(\zeta)G(\xi - \zeta)d\zeta \approx \sum_{j=0}^{j_b - j_a} F_{j+j_a}G_{j+j_a-j_\xi}\Delta\zeta,$$

where j_c denotes the grid index of $\xi = c$. Here, we also use the same discretization of ζ as for ξ, so that $\Delta\zeta = \Delta\xi$. Thus, the derivatives of Φ can be written as follows

$$\begin{aligned}\Phi_\xi &= \sum_{j=0}^{j_1 - j_0} P_j^n \frac{\varphi_{2j+j_0-i-1}^n - \varphi_{2j+j_0-i+1}^n}{2\Delta\xi}\Delta\zeta = \frac{1}{2}\sum_{j=0}^{j_1 - j_0} P_j^n(\varphi_{2j+j_0-i-1}^n - \varphi_{2j+j_0-i+1}^n)\\ \Phi_{t_1} &= \sum_{j=0}^{j_1 - j_0}\left[\frac{P_j^{n+1} - P_j^n}{\Delta t_1}\varphi_{2j+j_0-i}^n\Delta\zeta + P_j^n\frac{\varphi_{2j+j_0-i}^{n+1} - \varphi_{2j+j_0-i}^n}{\Delta t_1}\Delta\zeta\right]\\ &= \frac{\Delta\xi}{\Delta t_1}\sum_{j=0}^{j_1 - j_0}(P_j^{n+1} - P_j^n)\varphi_{2j+j_0-i}^n + P_j^n(\varphi_{2j+j_0-i}^{n+1} - \varphi_{2j+j_0-i}^n),\end{aligned}$$

where

$$P_j^n = \frac{\varphi_{j+j_0+1}^n - 2\varphi_{j+j_0}^n + \varphi_{j+j_0-1}^n}{(\Delta\zeta)^2} + \frac{\varphi_{j+j_1-1}^n + 2\varphi_{j+j_1}^n + \varphi_{j+j_1-1}^n}{(\Delta\zeta)^2}.$$

A similar equation can be derived for the computation of ψ in the domain $D_\eta = [\eta_{min}, \eta_{max}] \times [0, T_1]$, that is, $\psi_i^n = \psi(\eta_{min} + i\Delta\eta, n\Delta t_1)$, $\Delta\eta = \frac{\eta_{max}-\eta_{min}}{N_\eta}$, and

$$\psi(\xi, t_1 + \Delta t_1) = \psi(\xi, t_1) - \frac{\Delta t_1 \lambda}{2}\left(\psi_\xi^2(\xi, t_1) - \Psi(\xi, t_1)\right) + \frac{\lambda(\Delta t_1)^2}{4}\left(\lambda(\varphi_\xi^2\varphi_{\xi\xi} - \varphi_\xi \Psi_\xi) + \Psi_{t_1}\right) + \mathcal{O}((\Delta t_1)^3), \tag{B.4}$$

where

$$\Psi_{t_1}(\eta, t_1) = \int_0^1 [\psi_{\zeta\zeta}(\zeta, t_1) + \psi_{\zeta\zeta}(\zeta + 1, t_1)]\psi(2\zeta - \eta, t_1)d\zeta.$$

We use the same grid setup for η as for ξ, i.e. $\Delta\eta = \Delta\xi$. The schemes are applied up to time step N_{t_1} using the initial conditions

$$\varphi_i^0 = \varphi(\xi, 0), \qquad \psi_i^0 = \psi(\xi, 0),$$

and the boundary conditions

$$\varphi_{j_0}^n = \varphi_{j_2}^n, \qquad \psi_{j_0}^n = \psi_{j_2}^n. \tag{B.5}$$

The initial conditions can be computed by using (22), yielding

$$\varphi_i^0 = \frac{1}{2}\left(f(i\Delta\xi) - \sum_{j=0}^{j_i} g(j\Delta\xi)\right), \qquad \psi_i^0 = \frac{1}{2}\left(f(i\Delta\eta) + \sum_{j=0}^{j_i} g(j\Delta\eta)\right). \tag{B.6}$$

It should be kept in mind that the spatial indices of φ or ψ, especially in the Riemann sum, may have values outside the defined (x, t) discretization domain. In this case, we can use the periodicity properties, i.e. $\varphi_{j_a}^n = \varphi_{j_a+j_2}^n$, to make sure that the computations are correct inside the defined domain.

We also want to obtain the numerical solution for $\tilde{v}^{[1]}$, which satisfies

$$\tilde{v}^{[1]}(x, t_0, t_1) = \varphi(x - t_0, t_1) + \psi(x + t_0, t_1).$$

To compute $\tilde{v}^{[1]}$ in a domain $D_v = [0, X] \times [0, T]$, we have to compute φ and ψ in the following domain

$$D_\varphi = [-T, X] \times [0, T_1], \quad D_\psi = [0, T + X] \times [0, T_1]. \tag{B.7}$$

Wrapping up, we formulate the following procedure:

1. compute φ_i^0 and ψ_i^0 using (B.6) for all values of i in the respective domains;
2. for all values of $n = 0 \dots N_t - 1$,
   (a) compute φ_i^{n+1} and ψ_i^{n+1} using (B.3) and (B.4) for i from 1 to $N_\xi - 1$ or $N_\eta - 1$;
   (b) set values for the boundary points N_ξ and N_η using (B.5);
3. for $i = 0 \dots N_\xi$ and $j = 0 \dots N_\eta$,
   (a) introduce indices for the discretization of (B.7);
   (b) transform the (ξ, η)-coordinates back to the (x, t)-coordinates;
   (c) compute $\tilde{v}^{[0]}(x, t_0, t_1)$ from $w^{[0]}(\xi, \eta, t_1)$.

B.2. The forward-time center-space method for the original system (3a)–(3d)

Consider the original system (3a)–(3d). Recall that actually $u(x, \tau) = y(x) + \varepsilon v(x, \tau)$ and $t = \tau(1 - s_y)$. Our goal is to compare the numerical results for v by using the characteristic coordinates with the numerical results for the original system. Thus, our (x, t)-computation domain now should be $D_v = [0, 1] \times [0, T]$. We apply a similar domain of discretization as before. We denote $v_i^n = v(i\Delta x, n\Delta t)$ and $s^n = s(n\Delta t)$. We apply center finite difference scheme and obtain an explicit equation for v_i^{n+1}. Boundary conditions and initial conditions are treated in the usual way. Also, the function $s(t)$ is treated as an unknown function satisfying the given initial conditions.

Wrapping up, we can compute v and s for each i and n by the following procedure:

1. Compute $v_i^0 = f(i\Delta x)$ for $i = 0 \dots N_x - 1$;
2. Compute s^1 and v_i^1 by using the boundary and initial conditions for $i = 1 \dots N_x - 1$;
3. For all values of $n = 1 \dots N_t - 1$,
   (a) determine the boundary points v_0^n and $v_{N_x}^n$ by using the boundary conditions;
   (b) compute s^{n+1} by using a time-step Δt;
   (c) compute v_i^{n+1} by using a time-step Δt for $i = 1 \dots N_x - 1$.

References

[1] N.L. Balazs, On the solution of the wave equation with moving boundaries, J. Math. Anal. Appl. 3 (3) (1961) 472–484, http://dx.doi.org/10.1016/0022-247X(61)90071-3.
[2] C. Issanchou, J.-L. Le Carrou, S. Bilbao, C. Touzé, O. Doaré, A Modal Approach to the Numerical Simulation of a String Vibrating against an Obstacle: Applications to Sound Synthesis, in: 19th International Conference on Digital Audio Effects, DAFx-16, Brno, Czech Republic, 2016, pp. 1–8.
[3] B. Pelloni, D. Pinotsis, Moving boundary value problems for the wave equation, J. Comput. Appl. Math. 234 (6) (2010) 1685–1691, http://dx.doi.org/10.1016/j.cam.2009.08.016.
[4] D. Kartofelev, Kinematics of ideal string vibration against a rigid obstacle, in: 20th International Conference on Digital Audio Effects, DAFx-17, Edinburgh, UK, 2017, pp. 40–47.
[5] S. Bilbao, Numerical modeling of string barrier collisions, in: Proceedings of the International Symposium on Musical Acoustics, 2014, International Symposium on Musical Acoustics ISMA 2014 ; Conference date: 07-07-2014 Through 12-07-2014.
[6] C. Issanchou, V. Acary, F. Pérignon, C. Touzé, J.-L. Le Carrou, Nonsmooth contact dynamics for the numerical simulation of collisions in musical string instruments, J. Acoust. Soc. Am. 143 (5) (2018) 3195–3205, http://dx.doi.org/10.1121/1.5039740.
[7] C.P. Vyasarayani, S. Birkett, J. McPhee, Modeling the dynamics of a vibrating string with a finite distributed unilateral constraint: Application to the sitar, J. Acoust. Soc. Am. 125 (6) (2009) 3673–3682, http://dx.doi.org/10.1121/1.3123403.
[8] A. Mandal, P. Wahi, Natural frequencies, modeshapes and modal interactions for strings vibrating against an obstacle: Relevance to Sitar and Veena, J. Sound Vib. 338 (2015) 42–59, http://dx.doi.org/10.1016/j.jsv.2014.06.010.
[9] A. Mandal, P. Wahi, Mode-locking and improved harmonicity for real strings vibrating in the presence of a curved obstacle, Nonlinear Dynam. 88 (2017) 2203–2224, http://dx.doi.org/10.1007/s11071-017-3371-y.
[10] H. Singh, P. Wahi, Role of curvatures in determining the characteristics of a string vibrating against a doubly curved obstacle, J. Sound Vib. 402 (2017) 1–13, http://dx.doi.org/10.1016/j.jsv.2017.04.043.
[11] H. Singh, A.K. Mandal, P. Wahi, Non-planar motions of a string vibrating against a smooth unilateral obstacle, MATEC Web Conf. 83 (2016) 01010, http://dx.doi.org/10.1051/matecconf/20168301010.
[12] A.K. Mandal, P. Wahi, Equipartition of modal energy in an ideal string vibrating in the presence of a boundary obstacle, Nonlinear Dynam. (2023) 1–18.
[13] R.A. Malookani, W.T. van Horssen, On the asymptotic approximation of the solution of an equation for a non-constant axially moving string, J. Sound Vib. 367 (2016) 203–218, http://dx.doi.org/10.1016/j.jsv.2015.12.043.
[14] Darmawijoyo, W.T. van Horssen, P. Clément, On a Rayleigh wave equation with boundary damping, Nonlinear Dynam. 33 (2003) 399–429, http://dx.doi.org/10.1023/B:NODY.0000009939.57092.ad.